JOURNAL OF Materials CHEMISTRY

High-pressure synthesis of Ga-substituted $LiCoO_2$ with layered crystal structure

Radostina Stoyanova,*[a] Ekaterina Zhecheva,[a] Geoffrey Bromiley,[b] Tiziana Boffa Ballaran,[b] Ricardo Alcántara,[c] Juan-Isidro Corredor[c] and José-Luis Tirado[c]

[a]*Institute of General and Inorganic Chemistry, Bulgarian Academy of Sciences, 1113 Sofia, Bulgaria. E-mail: radstoy@svr.igic.bas.bg; Fax: +359 2 705024; Tel: +359 2 9793582*
[b]*Bayerisches Geoinstitut, Universität Bayreuth, D-95440 Bayreuth, Germany*
[c]*Laboratorio de Química Inorgánica, Edificio C3. Primera planta, Campus de Rabanales, Universidad de Córdoba, 14071 Córdoba, Spain*

Received 28th January 2002, Accepted 23rd April 2002
First published as an Advance Article on the web 7th June 2002

$LiGa_yCo_{1-y}O_2$ solid solutions with a layered crystal structure ($0 \leqslant y < 0.75$) were prepared under high-pressure (3 GPa) at 850 °C using a piston–cylinder type apparatus. This is in contrast to the solubility of Ga in the layered $LiCoO_2$ structure at atmospheric pressure, which is strongly limited, and reaches a maximum value of $y = 0.1$ at 700 °C. The structure of Ga substituted $LiCoO_2$ is characterized by XRD analysis and IR spectroscopy. It has been found that Ga substitutes for Co in the CoO_2 layer (3a site), while Li and O are in their normal positions (3b and 6c, respectively). The progressive replacement of Co by Ga leads to a linear increase in the mean M–O bond distance and to a smooth decrease in frequency of the main vibration of the $Ga_yCo_{1-y}O_2$ layer, thus indicating a random Co/Ga distribution. The electrochemical performance of $LiGa_yCo_{1-y}O_2$ as a cathode material in lithium ion cells has been evaluated in potentiostatic and galvanostatic experiments. The de-intercalation voltage of the $LiGa_yCo_{1-y}O_2$ solid solutions increases and the reversible capacity decreases with increasing gallium content.

Introduction

The use of $LiCoO_2$ oxides as an advanced cathode material in lithium-ion batteries has motivated numerous studies on their solid state chemistry.[1–4] Recently, replacement of Co by non-transition metal ions (such as B, Mg, Al *etc.*) has been found to have a significant effect on the electrochemical behavior of substituted $LiCoO_2$.[5–16] Since non-transition metal ions do not participate in the electrochemical reaction, the original specific capacity of substituted $LiCoO_2$ is lower than that of pure $LiCoO_2$. However, the main features of the doped materials are an improved thermal stability in the delithiated state and a low capacity fade when cycled to high potentials.

The interplay between the geometric and electronic structure of elements determines the formation of $LiM_yCo_{1-y}O_2$ solid solutions. For example, Mg and B dopants display a limited solubility in $LiCoO_2$ (upto 10 and 5%, respectively), while the aptitude of $LiCoO_2$ to dissolve Al reaches up to 80%.[6–8,16] However, an improved cycling stability has been found for $LiCoO_2$ doped with B and Mg,[6–9] while Al doping has a negative effect on the capacity retention of $LiCoO_2$.[10–15] The most important feature of Al dopants is the increased potential for Li extraction as compared with pure $LiCoO_2$.[12–14] Using *ab initio* calculations based on the ultrasoft-pseudopotential method, it has been predicted that lithium intercalation/de-intercalation will take place with the participation of oxygen rather than cobalt.[10]

Following these considerations, one can expect changes in the crystal chemistry and electrochemistry of $LiCoO_2$ when Co is partially replaced by the larger Ga. $LiCoO_2$ displays an ordered rock-salt structure, in which Co and Li separately occupy the two octahedral positions in the (111) cubic planes (3a and 3b sites), thus leading to the formation of distinct LiO_2 and CoO_2 layers ($R\bar{3}m$ space group).[17] A similar crystal structure has been found for α-$LiGaO_2$ by Marezio and Remeika.[18] However, the layered modification of $LiGaO_2$ can only be obtained at high pressures (3 GPa, 850 °C). At atmospheric pressure, the stable structural modification of $LiGaO_2$ is the γ-form where Li and Ga occupy tetrahedral sites.[19] There is also a third structural modification of $LiGaO_2$, which is an intermediate product of the pressure-induced transformation of the γ- into the α-form (1.8 GPa and 420 °C). To the best of our knowledge, there are no data on the synthesis of $LiGa_y$-$Co_{1-y}O_2$ solid solutions having a layered crystal structure.

In the present work, data on the formation of a solid solution of $LiCoO_2$ with $LiGaO_2$ under high pressure are provided. The structure and electrochemistry of Ga-substituted $LiCoO_2$ are characterized by XRD analysis, IR spectroscopy and galvanostatic/potentiostatic experiments.

Experimental

Acetate hydroxide precursors were used for the preparation of the Ga-substituted oxides. Ga_2O_3 (Fluka) was dispersed in a LiOH solution under continuous stirring for 1 d at 50 °C. After that, $Co(CH_3COO)_2 \cdot 4H_2O$ (Fluka) was added to the suspension. The ratio between the components was as follows: Li/(Co + Ga) = 1.02 and Ga/(Co + Ga) = y, $0 \leqslant y \leqslant 1$. After ageing for 1 d, the acetate hydroxide precipitates were cooled to room temperature, then frozen instantly with liquid nitrogen, and dried under vacuum (20–30 mbar) at −20 °C with an Alpha-Crist freeze-dryer (Germany). After drying, the solid residues were decomposed by heating from room temperature to 600 °C with a heating rate of 1° min^{-1} for 5 h. Samples were then synthesised at 850 °C at 3 GPa for 5 to 15 h. The Ga-substituted oxides thus prepared were olive-green coloured. For the sake of comparison, some experiments were carried out under atmospheric pressure at 600 and 700 °C for 24 h in air.

High-pressure synthesis was carried out in a 1/2 inch end-loaded piston–cylinder apparatus at the Bayerisches Geoinstitut. Samples were encapsulated in 1 cm long, 5 mm diameter welded Pt capsules. The capsules were surrounded by a pyrophyllite sample holder and inserted into talc–Pyrex cells

DOI: 10.1039/b201030e

with a tapered graphite resistance heater. Pressure was calibrated against the quartz–coesite and kyanite–sillimanite transitions, as well as the melting point of diopside. The temperature was measured with a $Pt_{90}Rh_{10}$–Pt thermocouple. Experiments were performed using the "hot-piston in" technique. In this method, the pressure is increased to approximately 10% below the final run pressure, then the temperature is increased to the desired run temperature, and finally, the pressure is increased to the final value. The samples were quenched isobarically by turning off the power whilst maintaining a pressure within 0.02 GPa of the run pressure. Quench rates were of the order of 75 °C s^{-1}.

X-ray phase analysis was carried out on a D5000-Siemens diffractometer using Cu Kα radiation. X-ray powder diffraction for Rietveld refinement was performed with a STOE Stadi/P diffractometer, Co $K\alpha_1$ radiation, with a Si internal standard. The scan range $10 \leqslant 2\theta \leqslant 110$ in a step increment of 0.02° was utilized. The computer program FULLPROF was used for the calculation.[20] The diffractometer point zero, Lorentzian/Gaussian fraction of the pseudo-Voigt peak function, scale factor, lattice constants (*a* and *c*), oxygen parameter (*z*), thermal factors for 3a, 3b and 6c positions, halfwidth parameters, preferred orientation and asymmetry parameters were refined. The refinement model considers two phases: (i) a layered phase ($R\bar{3}m$ space group and atomic positions 3a (0,0,0); 3b (0,0,0.5) and 6c (0,0,*z*)); (ii) an impurity phase of cubic spinel ($Fd3m$ space group and atomic positions 8a (0,0,0); 16d ($\frac{5}{8}$, $\frac{5}{8}$, $\frac{5}{8}$) and 32e (≈0.389, ≈0.389, ≈0.389)). To gain stability during the two-phase refinement, a Ga/(Co + Ga) ratio imposed by the chemical composition of the precursors was used: $LiGa_yCo_{1-y}O_2$ and $Ga_yCo_{3-y}O_4$, respectively. Subsequently, the cationic occupancy factors were refined taking into account that the total occupancies of the 3a and 3b sites are equal to unity.

The infrared spectra were recorded on a NICOLET AVATAR-320 spectrometer in KBr pellets.

Electrochemical experiments were carried out in Swagelok-type cells using a MacPile system in galvanostatic and potentiostatic mode. The positive electrode was formed by active material (85%), Carbon Black and graphite (10%), and PVDF (5%). The negative electrode was Li. The electrolyte was $LiPF_6$ dissolved in EC : DEC supplied by Merck, which soaked Whatman and Celgard separators. Cells were made in a dry box with Ar atmosphere containing less than 1 ppm of oxygen and water. In order to normalize the potentiostatic results, the current intensities are expressed as mA g^{-1} of electrode active material.

Results and discussions

Structural characterization of $LiGa_yCo_{1-y}O_2$

XRD patterns demonstrate that the high-pressure synthesis yielded Ga-substituted $LiCoO_2$ oxides with a layered crystal structure up to $y = 0.75$ (Figs. 1, 2). However, an impurity

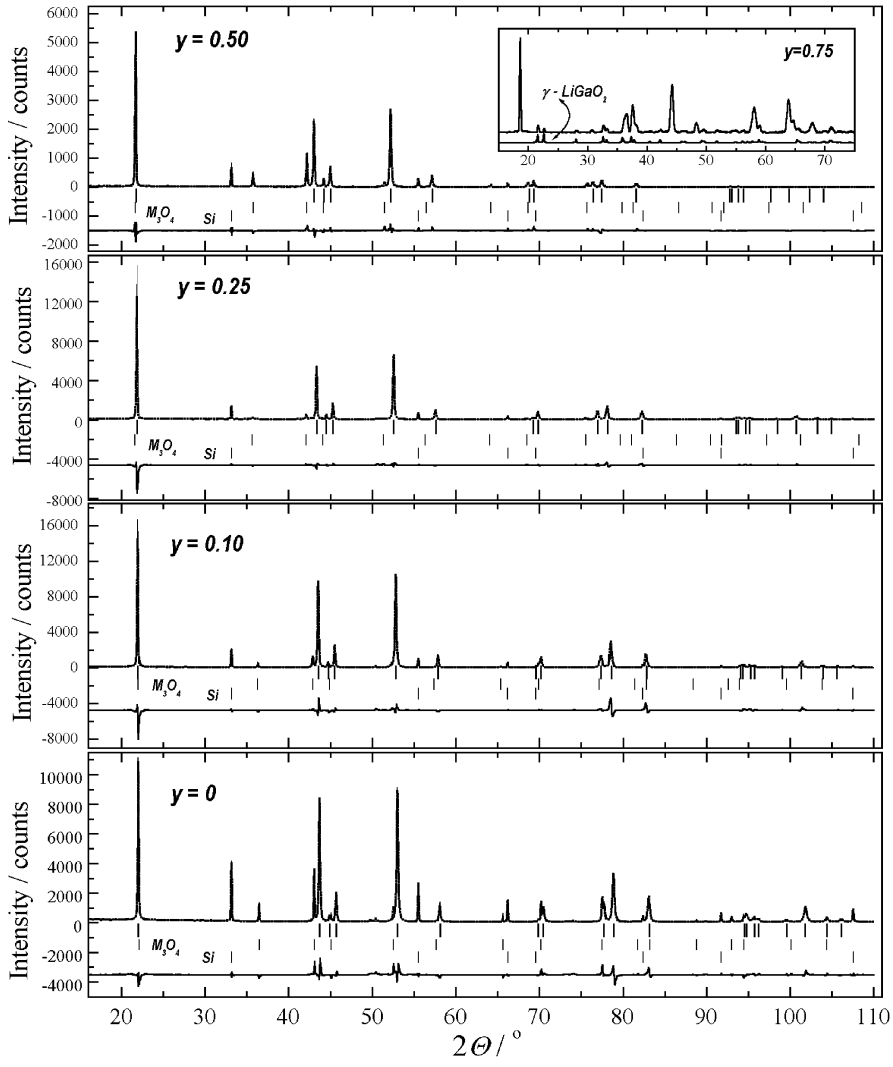

Fig. 1 XRD patterns of $LiGa_yCo_{1-y}O_2$ synthesised at high pressure (Co $K\alpha_1$-radiation). The difference between the observed and calculated profiles is plotted. Bragg reflections for layered $LiGa_yCo_{1-y}O_2$, impurity spinel phases and Si standard are indicated. The inset presents the XRD patterns of the composition with $y = 0.75$ obtained at 3 GPa and of γ-$LiGaO_2$ obtained at atmospheric pressure (Cu Kα radiation is used).

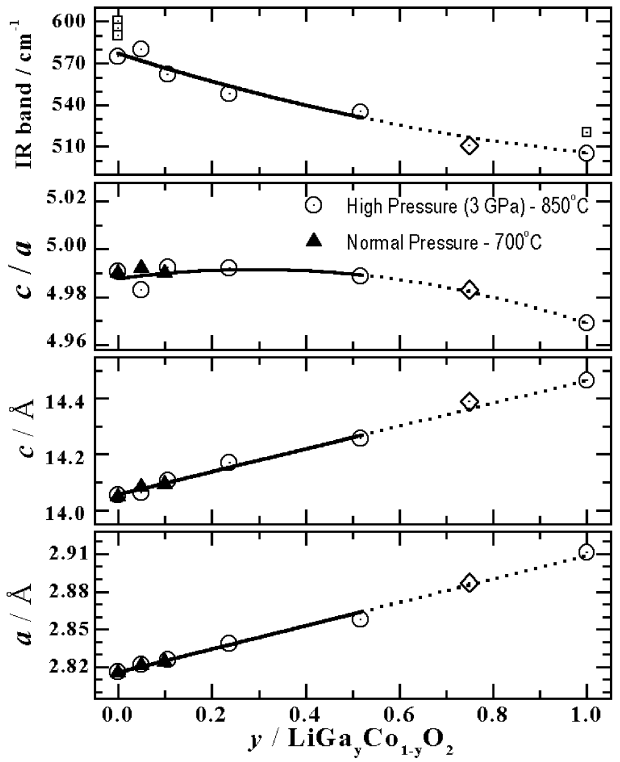

Fig. 2 Unit cell parameters and the most intense IR band *vs.* Ga content for $LiGa_yCo_{1-y}O_2$ solid solutions synthesised under high and atmospheric pressure. The diamond label at $y = 0.75$ indicates that the galium content was taken from the precursor composition. Square labels correspond to the data from refs. 21 and 22.

phase having a spinel composition has been detected for all samples studied and its amount varies between 1 and 5 wt.% (Table 1). The weight fraction of this impurity spinel phase decreases with pressure (from 3 to 0.5 GPa), as well as with increasing Li/Co ratio in the precursor (from 1.02 to 1.10). By increasing the Ga content up to $y = 0.25$, the spinel lattice parameter increases, after which a slight decrease in a is observed. Since CoO and Ga_2O_3 form a normal spinel, $CoGa_2O_4$ ($a = 8.325$ Å, JCPDS Powder Diffraction File 11-0698), the observed changes in the spinel lattice parameter indicate incorporation of Ga into the Co_3O_4 spinel. An accurate determination of the Ga/Co ratio in the spinel phases is obscure due to their low percentage abundance. It is not clear why this impurity spinel phase has been formed since, at atmospheric pressure, the LiCo-precursors give a $LiCoO_2$ monophase only. However, the important consequence from these results is a constancy in unit cell parameters of the main $LiCoO_2$ phase irrespective of the pressure and the initial Li/Co ratio used. It appears that the solubility of Ga in $LiGa_yCo_{1-y}O_2$ is lower than $y = 0.75$ (Fig. 1). Contrary to the high-pressure synthesis, the incorporation of Ga into the layered structure of $LiCoO_2$ at atmospheric pressure is strongly limited and depends on the preparation temperature: at 600 and 700 °C the Ga solubility reaches up to $y < 0.25$ and 0.10, respectively. This means that Ga-rich oxides obtained under high pressures are metastable phases and, during reheating in air, dissociate to Ga-poor $LiCoO_2$ and orthorhombic γ-$LiGaO_2$.

One reason for the stabilization of the layered structure of $LiCoO_2$ is the difference in size between Li^+ and Co^{3+}; 0.76 and 0.54 Å, respectively. The incorporation of Ga into $LiCoO_2$ produces a linear expansion of the unit cell dimension (Vegard's behaviour), in accordance with the higher ionic radius of Ga^{3+} as compared to that of Co^{3+}, 0.62 Å (Fig. 2). The *c*/*a* ratio, which gives the extent of the trigonal distortion, remains nearly unchanged for compositions with $y < 0.5$, after which a slight decrease in *c*/*a* is observed. Hence, a layered crystal framework is preserved for $LiGa_yCo_{1-y}O_2$ with $y < 0.75$ irrespective of the fact that the larger Ga replaces the smaller Co. According to the structural refinement (Table 1), Ga substitutes for Co in the CoO_2 layer (3a site), while Li and O are in their normal positions (3b and 6c, respectively). The refined occupancy factors for the 3a site are given in Table 1. The progressive replacement of Co by Ga causes a linear increase in the mean M–O bond distance, indicating a random Co/Ga distribution (Table 1). On the other hand, the Li–O bond distance displays a uniform increase upon Ga substitution, which is a consequence of the different extent of trigonal distortion of the layered structure for $LiCoO_2$ and $LiGaO_2$.

An IR spectroscopic study of $LiGa_yCo_{1-y}O_2$ gives additional information on the $Ga_yCo_{1-y}O_2$ layer formation. According to the factor group analysis, the active IR modes for the trigonal structure are four, including the stretching and bending vibrations of MO_6 octahedra.[21–22] Since metal octahedra in the layer share a common edge, the observed frequencies can be related to the whole vibration of the layer, not to a single M–O bond.[21] The difference in stretching forces for Li and Co is the reason for the separation of the LiO_2 and Co/GaO_2 vibrations (two-mode behaviour). As a result, the predicted modes are doubled; in the 400–700 cm^{-1} region there are bands due to Co/GaO_2 vibrations, whereas LiO_2 vibrations are within the region 200–400 cm^{-1}. Fig. 3 shows the IR spectra of $LiGa_yCo_{1-y}O_2$ in the 400–900 cm^{-1} region, where only the $Ga_yCo_{1-y}O_2$ vibrations are visible. To help understand the effect of the impurity spinel phase on the IR spectra of $LiGa_yCo_{1-y}O_2$, some references for the IR spectra of Co_3O_4 spinel and of layered $LiCoO_2$ (obtained at normal pressure) are presented in Fig. 3. The spinel phase is characterized by two peaks at 565 and 660 cm^{-1}. The layered $LiCoO_2$ phase exhibits three intense peaks at 517, 555 and 595 cm^{-1} together with smaller features at 615 and 648 cm^{-1}. For Ga-poor compositions, three main IR bands can be distinguished, while for the Ga-rich compositions the IR bands are broken into several components. Irrespective of the different IR profiles observed for Ga-poor and Ga-rich compositions, the change in position of the most intense IR component seems to be consistent with the expansion of the cell dimension caused by the progressive replacement of Co by Ga. This enables one to associate the most intense IR band with the stretching vibration of MO_6 octahedra. Fig. 2 gives the dependence of the

Table 1 Structural parameters determined from XRD pattern Rietveld refinement for $LiGa_yCo_{1-y}O_2$ synthesised at high pressure (3 GPa)

	Layered phase, $R\bar{3}m$ space group								Spinel phase, $Fd3m$ space group	
y	a/Å (± 0.00008)	c/Å (± 0.0004)	z, oxygen parameter	$y_{refined}$, 3a site	B_{iso} (3a)/Å^2	R_B (%)	Mean M–O/Å	Li–O/Å	a ± 0.0001	Weight fraction
0.0	2.81602	14.0535	0.2591(6)	0	0.44(8)	7.81	1.932	2.081	8.0819	0.041
0.10	2.82547	14.1060	0.2589(5)	0.106(9)	0.28(8)	7.46	1.940	2.087	8.1129	0.019
0.25	2.83854	14.1701	0.2594(3)	0.238(3)	0.32(6)	3.77	1.945	2.101	8.2585	0.019
0.50	2.85760	14.2558	0.2578(6)	0.518(9)	0.63(12)	7.43	1.970	2.100	8.2423	0.052
1.0[18]	2.9113	14.466	0.2583	—	—	—	2.00	2.14		

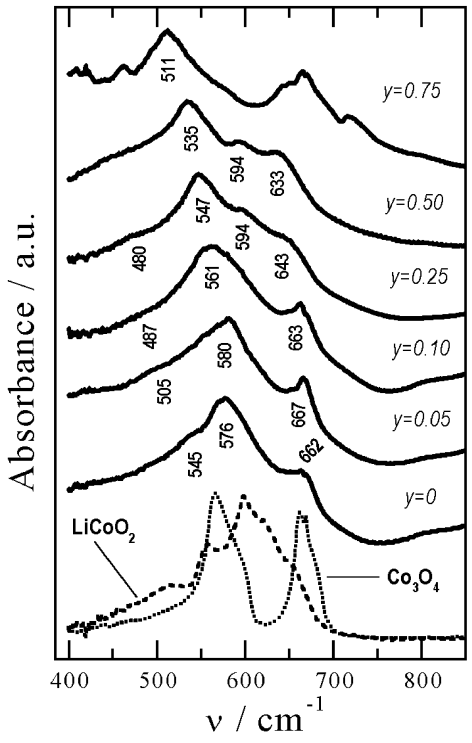

Fig. 3 IR spectra of $LiGa_yCo_{1-y}O_2$ solid solutions synthesised under high pressure. For the sake of comparison, the IR spectra of Co_3O_4 spinel and layered $LiCoO_2$ are also given.

most intense IR band on the Ga content in $LiGa_yCo_{1-y}O_2$. It appears that the band position decreases as the mean M–O bond distance (determined by structural analysis, Table 1) increases, thus supporting the isomorphic substitution of Co by Ga in MO_2 layers.

Electrochemical lithium de-intercalation from and intercalation into $LiGa_yCo_{1-y}O_2$

The ability of $LiGa_yCo_{1-y}O_2$ to remove and insert lithium was evaluated in potentiostatic and galvanostatic experiments. The potentiostatic intermittent titration technique (PITT) results of $Li/LiCoO_2$ batteries are shown in Fig. 4. For pure $LiCoO_2$ charged between 2.5 and 4.5 V, the highest reversible capacity (138 mAh g^{-1}) is observed for a sample obtained at 3 GPa using a Li/Co ratio equal to 1.10. The higher capacity observed for $Li_{1.1}CoO_2$-30 as compared to $LiCoO_2$-30 can be associated with the lower content of the impurity spinel phase for the former sample. In fact, the reversible capacities reported for $LiCoO_2$ are usually lower than 130 mAh g^{-1}. Regarding the intensity *vs.* voltage curve, the main oxidation peak is observed at *ca.* 4.1 V, and the main reduction peak at *ca.* 3.8 V. These effects correspond to the redox couple Co^{3+}/Co^{4+} and are accompanied by a significant expansion of the *c* parameter during lithium extraction.[23] In the derivative curve of the galvanostatic experiment at a C/50 rate (Fig. 5A), the curve profile is similar to the PITT results. In addition, two small peaks are observed at higher voltage that can be assigned to an order–disorder transition of Li^+ ions in the interlayer free of "alien" atoms.[5] These results demonstrate a similar electrochemical behavior of $LiCoO_2$ obtained at normal and at high pressure. It appears that the impurity spinel phase does not

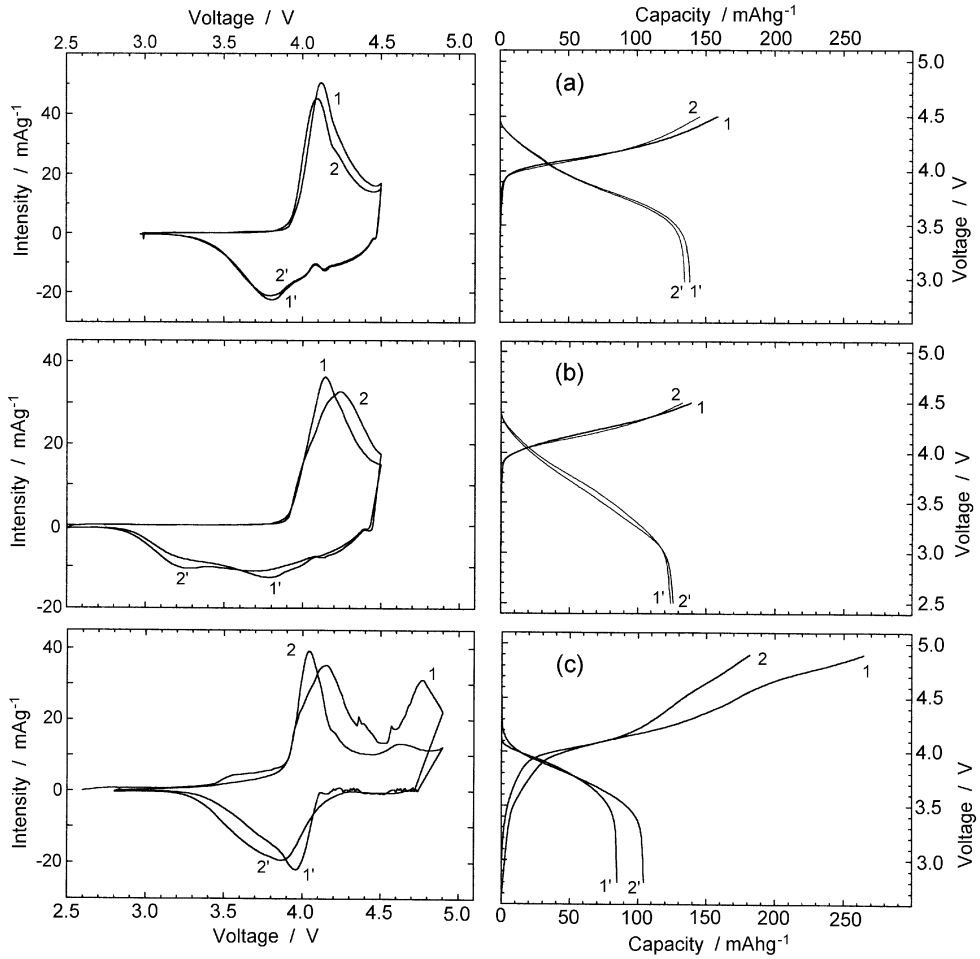

Fig. 4 PITT results for the first two charge (1, 2)/discharge(1′, 2′) cycles of $Li/LiPF_6/Li_xCoO_2$ batteries, using cathode materials obtained at high pressure for: (a) $Li_{1.1}CoO_2$ at 3 GPa, (b) $LiCoO_2$ at 3 GPa and (c) $LiCoO_2$ at 0.5 GPa. Speed rate: 10 mV (0.1 h)$^{-1}$.

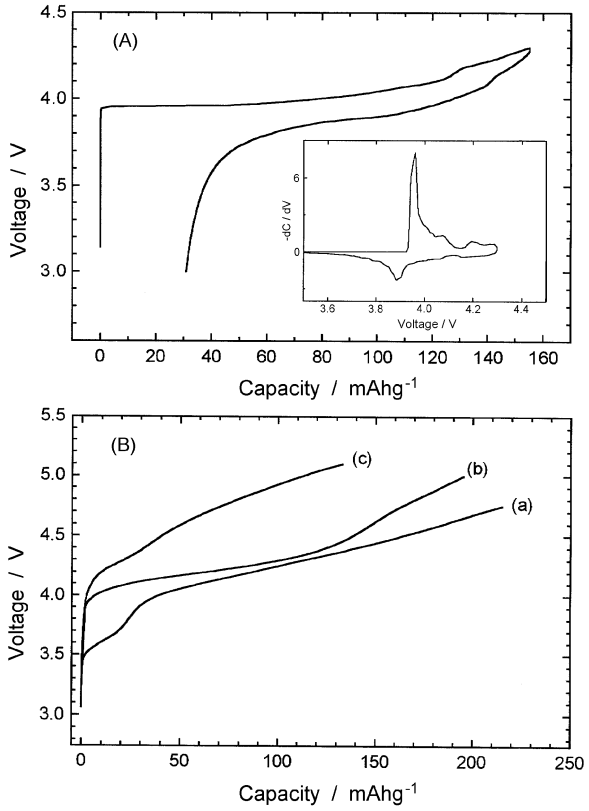

Fig. 5 (A) Galvanostatic charge/discharge cycle at C/50 of a Li/$LiPF_6$/Li_xCoO_2 battery using like cathode $Li_{1.1}CoO_2$ obtained at 3 GPa. The corresponding derivative curve is shown as an inset. (B) Comparison of voltage *vs.* capacity for the first potentiostatic charge of $LiGa_yCo_{1-y}O_2$/$LiPF_6$/Li batteries for (a) $y = 0.05$, (b) $y = 0.10$ and (c) $y = 0.25$. Measurements were carried out at 10 mV $(0.1\ h)^{-1}$ at room temperature.

contribute to the electrochemical performance of high-pressure $LiCoO_2$.

By raising the upper voltage limit to 4.9 V, complete extraction of Li from $LiCoO_2$ is reached and the de-intercalation curve shows a second peak at about 4.8 V (Fig. 4c). After the discharge to 2.8 V, only one broad peak is resolved during the intercalation of Li. The observed charge/discharge curve profiles for high-pressure $LiCoO_2$ resemble that for $LiCoO_2$ obtained under normal pressure.[24–26] The profile of the charge/discharge curve of $LiCoO_2$ has been shown to depend on the voltage range where lithium intercalation/deintercalation takes place.[24] The high voltage plateau is thought to be due to a two-phase reaction with the formation of $\square CoO_2$. The intercalation of Li into $\square CoO_2$ proceeds *via* several structural transformations, which are irreversible and cause changes in the discharge curve profile.[24,25] By analogy, it seems that the same mechanism operates for $LiCoO_2$ obtained under high pressure (Fig. 4c). However, in addition to internal stresses and "electrochemical grinding" at high voltage, a contribution from the electrolyte decomposition to the loss of capacity upon cycling cannot be discarded. From these results one may conclude that the electrochemical properties of $LiCoO_2$ obtained at high pressure are close to that of $LiCoO_2$ obtained at normal pressure.

The similar electrochemical performances of $LiCoO_2$ obtained at normal and at high pressures allow us to outline the effect of Ga on the lithium de-intercalation from and intercalation into Ga-substituted oxides. Fig. 5B compares the "voltage *vs.* capacity" curves for the first charge of $LiGa_yCo_{1-y}O_2$ solid solutions. One can see that the first voltage plateau at 4 V, observed for pure $LiCoO_2$, becomes less pronounced upon Ga doping. For samples charged to a close depth, it appears that the voltage of the first charge increases with the amount of Ga doping. For the $Li_xAl_yCo_{1-y}O_2$ system, this was previously observed by Ceder *et al.*[10] in open circuit conditions in agreement with the predictions from *ab initio* calculations, and also by Alcántara *et al.*[11] Comparing the effect of Al and Ga, one may conclude that the charge voltage increases more rapidly for the Ga-substituted oxides. As a result of the increased charge voltage, the first charge capacity decreases upon Ga doping. When charging up to 5.1 V, the amount of extracted lithium decreases from 0.72 to 0.50 with a Ga content increasing from 0.10 to 0.25. During the first discharge up to 3.0 V, the subsequent lithium intercalation allows recovery of nearly half of the de-intercalted lithium (Fig. 6). The capacity retention decreases with Ga doping, similarly to the aluminium-containing samples. This may originate from the structural instability of Ga-substituted oxides caused most probably by the tendency of Ga to adopt tetra-coordination at

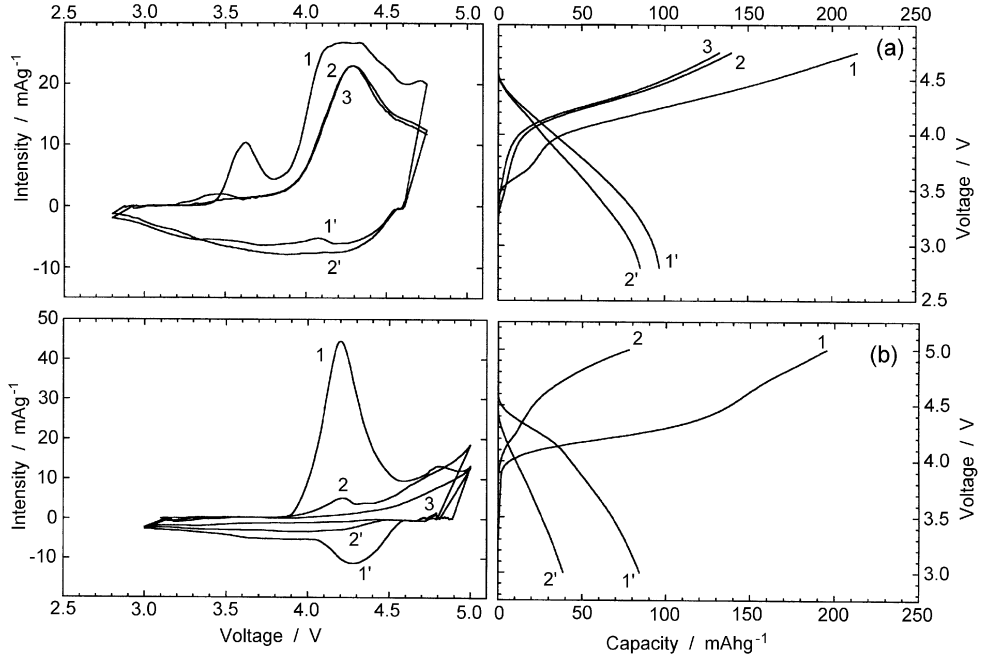

Fig. 6 First charge (1–3)/discharge(1′, 2′) PITT cycles of Li/$LiPF_6$/$LiGa_yCo_{1-y}O_2$ for (a) $y = 0.05$ and (b) $y = 0.10$.

normal pressure. In addition, a new peak is observed at about 3.6 V in the first charge for the sample with $y = 0.05$ (Fig. 6). The origin of this peak is not clear at present. Further studies on the structural stability of $LiGa_yCo_{1-y}O_2$ during lithium de-intercalation/intercalation are in progress.

Conclusions

High-pressure synthesis yields $LiGa_yCo_{1-y}O_2$ solid solutions with a layered crystal structure up to $y = 0.75$. At atmospheric pressure, the incorporation of Ga into the layered structure of $LiCoO_2$ is strongly limited, with a maximum value of $y = 0.10$ at 700 °C. It is shown that the larger Ga substitutes for the smaller Co in the CoO_2 layer (3a site), while Li and O are in their normal positions (3b and 6c, respectively). The progressive replacement of Co by Ga causes a linear increase in the mean M–O bond distance, indicating a random Co/Ga distribution. On the other hand, the Li–O bond distance displays a uniform increase with Ga substitution, which is a consequence of the different extent of trigonal distortion of the layered structures of $LiCoO_2$ and $LiGaO_2$. IR spectroscopy study on $LiGa_yCo_{1-y}O_2$ reveals that, between 400 and 700 cm^{-1}, the observed frequencies can be related to the vibration of the $Ga_yCo_{1-y}O_2$ layer. The position of the most intense IR band decreases as the mean M–O bond distance increases, thus supporting the isomorphic substitution of Ga for Co in MO_2 layers. Electrochemical examination shows identical electrochemical behaviour for $LiCoO_2$ obtained under atmospheric and high pressure. The de-intercalation voltage of the $LiGa_yCo_{1-y}O_2$ solid solutions increases and the reversible capacity decreases with increasing gallium content.

Acknowledgement

E. Zh. and R. S. acknowledge the National Science Fund of Bulgaria (Contract no. Ch810/1998) for financial support of the work concerning the synthesis at atmospheric pressure and the structural characterization of the oxides. R. S. is grateful to the EC for a grant of an EU "IHP–Access to Research Infrastructures" Programme (Contract No. HPRI-1999-CT-0004 to D. C. Rubie) in order to perform the high-pressure synthesis experiments at the Bayrisches Geoinstitute. R. A, J. I. C. and J. L. T. are grateful to MCYT for financial support (contract MAT99-0741).

References

1 P. Bruce, *J. Chem. Soc., Chem. Commun.*, 1997, 1817.
2 M. Winter, J. Besenhard, M. Spahr and P. Novak, *Adv. Mater.*, 1998, **10**, 725.
3 M. Brousesely, P. Biensan and B. Simon, *Electrochim. Acta*, 1999, **45**, 3.
4 R. Alcántara, P. Lavela, J.-L. Tirado, E. Zhecheva and R. Stoyanova, *J. Solid State Electrochem.*, 1999, **3**, 121.
5 J. N. Reimers, J. R. Dahn and U. von Sacken, *J. Electrochem. Soc.*, 1993, **140**, 2752.
6 R. Alcántara, P. Lavela, J. L. Tirado, R. Stoyanova and E. Zhecheva, *J. Solid State Chem.*, 1997, **134**, 265.
7 H. Tukamoto and A. R. West, *J. Electrochem. Soc.*, 1997, **144**, 3164.
8 M. Mladenov, R. Stoyanova, E. Zhecheva and S. Vassilev, *Electrochem. Commun.*, 2001, **3**, 410.
9 C. Julien, G. A. Nazri and A. Rougier, *Solid State Ionics*, 2000, **135**, 121.
10 G. Ceder, Y.-M. Chiang, D. R. Sadoway, M. K. Aydinol, Y.-I. Jang and B. Huang, *Nature*, 1998, **392**, 694.
11 R. Alcántara, P. Lavela, R. L. Relano, J.-L. Tirado, E. Zhecheva and R. Stoyanova, *Inorg. Chem.*, 1998, **37**, 264.
12 Y.-I. Jang, B. Huang, H. Wang, D. R. Sadoway, G. Ceder, Y.-M. Chiang, H. Liu and H. Tamura, *J. Electrochem. Soc.*, 1999, **146**, 862.
13 W.-S. Yoon, K.-K. Lee and K.-B. Kim, *J. Electrochem. Soc.*, 2000, **147**, 2023.
14 S.-T. Myung, N. Kumagai, Sh. Komaba and H.-T. Chung, *Solid State Ionics*, 2001, **139**, 47.
15 J. Cho, Y.-J. Kim and B. Park, *Chem. Mater.*, 2000, **12**, 3788.
16 E. Gaudin, F. Taulelle, R. Stoyanova, E. Zhecheva, R. Alcantara, P. Lavela and J. L. Tirado, *J. Phys. Chem. B*, 2001, **105**, 8081.
17 H. J. Orman and P. J. Wiseman, *Acta Crystallogr., Sect. C*, 1984, **40**, 12.
18 M. Marezio and J. P. Remeika, *J. Phys. Chem. Solids*, 1965, **26**, 1277.
19 M. Marezio, *Acta Crystallogr.*, 1965, **18**, 481.
20 J. Rodrigues-Carvajal, in *Satellite Meeting on Powder Diffraction of the XV Congress of the IUCr*, 1990, p. 127.
21 P. Tarte and J. Preudhomme, *Spectrochim. Acta, Part A*, 1970, **26**, 747.
22 R. Moore and W. White, *J. Am. Ceram. Soc.*, 1970, **53**, 679.
23 J. N. Reimers and J. R. Dahn, *J. Electrochem. Soc.*, 1992, **139**, 2091.
24 G. G. Amatucci, J. M. Tarascon and L. C. Klein, *Solid State Ionics*, 1996, **83**, 167.
25 G. G. Amatucci, J. M. Tarascon and L. C. Klein, *J. Electrochem. Soc.*, 1996, **143**, 1114.
26 M. Holzapfel, R. Schreiner and A. Ott, *Electrochim. Acta*, 2001, **46**, 1063.